Processing and Investigation Methods in Mechanochemical Kinetics

Evelina Colacino, Maria Carta, Giorgio Pia, Andrea Porcheddu, Pier Carlo Ricci, Francesco Delogu

ACS OMEGA

Article

Cite This: ACS Omega 2018, 3, 9196−9209

http://pubs.acs.org/journal/acsodf

Processing and Investigation Methods in Mechanochemical Kinetics

Evelina Colacino,*[,†] Maria Carta,[‡] Giorgio Pia,[‡] Andrea Porcheddu,[§] Pier Carlo Ricci,[∥] and Francesco Delogu*[,‡]

[†]Institut des Biomolécules Max Mousseron, Université de Montpellier, UMR5247 UM-CNRS-ENSCM, Place E. Bataillon, Campus Triolet cc1703, 34095 Montpellier Cedex 5, France

[‡]Dipartimento di Ingegneria Meccanica, Chimica, e dei Materiali, Università degli Studi di Cagliari, via Marengo 2, 09123 Cagliari, Italy

[§]Dipartimento di Scienze Chimiche e Geologiche, Università degli Studi di Cagliari, Cittadella Universitaria, SS 554 bivio per Sestu, 09042 Monserrato, Italy

[∥]Dipartimento di Fisica, Università degli Studi di Cagliari, Cittadella Universitaria, SS 554 bivio per Sestu, 09042 Monserrato, Italy

ABSTRACT: The present work focuses on the challenges that emerge in connection with the kinetics of mechanically activated transformations. This is an important topics to comprehend to enable the full exploitation of mechanical processing in a broad spectrum of areas related to chemistry and materials science and engineering. Emerging challenges involve a number of facets regarding materials and material properties, working principles of ball mills and milling conditions, and local changes occurring in series in processed materials. Within this context, it is highly desirable to relate the nature and rate of observed mechanochemical transformations to individual collisions and then to the processes induced by mechanical stresses on the molecular scale. Hence, it is necessary to characterize the milling regimes that can establish in ball mills regarding frequency and energy of collisions, map the relationship between milling dynamics and transformation kinetics, and obtain mechanistic information through proper time-resolved investigations *in situ*. A few specific hints are provided in this respect.

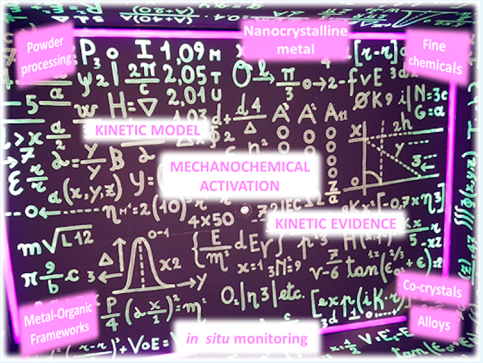

1. INTRODUCTION

The mechanical force of the ball milling (BM) technique is traditionally utilized in powder metallurgy and mineral processing to mix granular matter, reduce particle size, refine microstructure, and promote chemical reactivity.[1−4] The unit operation is based on the transfer of mechanical energy to powders during the collisions between milling tools that occur inside the reactor of a ball mill. Processes on the mesoscopic and microscopic scales occur impulsively in the volumes of powder mixture, which are trapped either between the colliding balls or between a ball and the reactor wall. The resulting mechanical deformation of powder particles can give rise to cold-welding and fracturing as well as to physical and chemical transformations.[1−4]

The nature and extent of local processes activated by individual collisions strictly depend on the nature of the processed powder. For instance, the BM of individual metals promotes the formation of a fine microstructure comprising crystalline grains with characteristic lengths between 5 and 50 nm.[5−8] Chemical effects associated with microstructural refinement emerge in the powder mixtures of elemental metals, where forced mixing on the atomic scale can result in the mechanical alloying of constituents.[1−4] Similarly, physical and chemical effects can be associated with the adequate mixing of molecular components which emerge in inorganic and organic synthesis[9−11] as well as in other areas of chemical and engineering research and technology. In this respect, crystal engineering represents a good example. Indeed, the use of mechanochemical methods has given further stimulus to the manufacturing of pharmaceutical co-crystals,[12−14] metal−organic frameworks (MOFs),[15] and deep-eutectic solvents.[15]

The increasing number of applications of mechanical activation to the synthesis of chemicals and the preparation of materials has recently driven a new, rapid surge of interest. As a consequence, the study of mechanically activated transformations is, presently, one of the most rapidly growing subjects in organic and materials chemistry. Yet, various menacing issues discourage attempts to transfer technology from the laboratory to industry. Milling dynamics has been characterized only in a few cases, and the kinetics and thermodynamics of mechanochemical transformations are still poorly understood.[1−4,16,17]

Within this context, in the present work we bring to the attention of researchers a few important facts: (1) Control of processing conditions is a necessary requisite to perform accurate kinetic studies. (2) The development of kinetic models is needed to relate experimental evidence to conversion processes involving much smaller time and length scales. (3)

Received: June 24, 2018
Accepted: July 30, 2018
Published: August 15, 2018

DOI: 10.1021/acsomega.8b01431
ACS Omega 2018, 3, 9196−9209

Direct information on such processes can be obtained by *in situ*, possibly time-resolved studies.

2. CHARACTERIZATION OF PROCESSING CONDITIONS

Ball mills involve simple working principles. The entire reactor, or part of it, undergoes periodic motion aimed at inducing collisions of the balls inside the reactor with each other and with the reactor walls.[1−4,18] The colliding surfaces of the milling media trap powder particles in between and subject them to mechanical loading. Non-hydrostatic mechanical stresses arise at every contact point between any pair of powder particles. Local collisional and frictional processes of variable intensity and duration take place at such locations.[19,20] Their occurrence, as well as their relative importance and intensity, depend on the milling conditions selected and the specific mechanical action of the ball mill.[1−4]

Working principles customarily allow ball mills to be divided into the two broad classes of mixers and attritors.[4] In mixers, balls collide at relatively high velocity, and impulsive dynamics dominates. In attritors, relatively low collision energy mostly results in frictional dynamics. However, it is worth noting that the modification of processing parameters makes it possible to move smoothly between the two milling regimes. Therefore, no rigid distinction between the two classes should be made.

Numerous factors affect processing conditions.[4] These include the mass of powder inside the reactor, the number and size of balls, the frequency of collisions and their energy, the temperature, the atmosphere inside the reactor, and the process control agents utilized to avoid or limit particle agglomeration. The effects of processing parameters on milling regimes have not yet systematically mapped.[1,21−24] However, the fragmentary information available from the literature indicates the powder charge, the number and size of balls, the frequency, and the energy of collisions as the most critical factors affecting the kinetics of mechanically activated transformations.[25−40]

Detailed characterization of the milling dynamics has been performed only for the SPEX Mixer/Mill 8000 and the Fritsch Pulverisette devices, respectively—the two most popular shaker and planetary mills. The SPEX Mixer/Mill 8000 allows processing powder charges of up to 30 mL. The reactor moves as schematically depicted in Figure 1, undergoing angular harmonic displacement in the vertical plane simultaneously with rotation in the equatorial plane. It typically works at a frequency of 14.6 Hz. The frequency range between 12.5 and 30.0 Hz[8,41] has been explored using a device equipped with a three-phase asynchronous motor controlled by a frequency converter.[29,30]

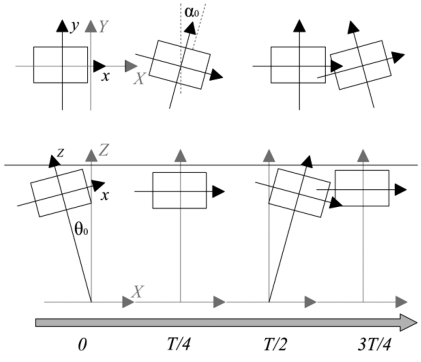

Figure 1. Schematic description of the reactor motion.

A methodology combining experimental and modeling studies allow characterizing the milling dynamics.[29,30,41] Collision frequency and energy can be accurately evaluated in the presence of both a single milling ball and a significant amount of powder using piezoelectric and magnetic sensors and high-speed video recording.[29,30,41] Two collisions per cycle take place, indicating that the ball alternately collides with the opposite reactor bases following relatively regular trajectories due to the energy dissipation during collisions.

In the absence of powder, and with a reactor frequency of about 18.3 Hz, a single milling ball 14 mm in diameter exhibits average collision frequency equal to about 89.3 Hz and a broad distribution of ball velocity with an average around 10.42 m s^{-1}. As powder charge is increased, collisions move from perfectly elastic to perfectly inelastic regimes. Accordingly, the average collision frequency on the reactor bases drops from 89.3 to 36.6 Hz, whereas the collision velocity on the reactor base decreases smoothly from 6 to 3 m s^{-1}.[42] In the case of perfectly inelastic collisions, the ball slides along the cylindrical wall, and collisions occur exclusively on the reactor bases. Two collisions per cycle take place, and the average collision velocity is equal to about 5.1 m s^{-1}. Collision velocity and milling frequency exhibit an approximately linear relationship.

The methodology mentioned above displays its whole potential when the mechanical treatment is performed with a single milling ball. However, numerical integration methods can be used to gain insight into milling regimes establishing in the presence of two or more balls.[42,43]

Information on the milling dynamics, although fragmentary, has also been given for planetary mills, which exhibit mechanical action and working conditions quite different from those arising in a shaker mill. These milling devices consist of one or more reactors lying in an eccentric position on a support disk. The disk and reactor rotate around their own axes in opposite directions, as shown in Figure 2. The two

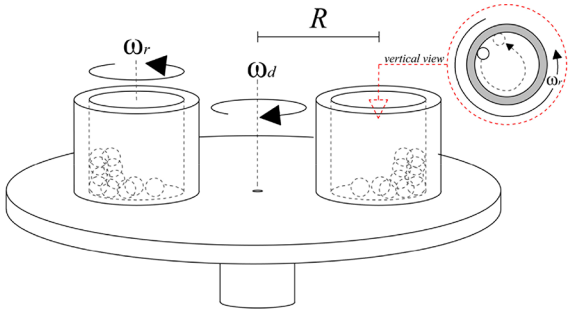

Figure 2. Schematic description of a planetary mill. The support disk rotates at an angular frequency ω_d, whereas the reactors, at distance R from the disk center, rotate in the opposite direction at an angular frequency ω_r. The typical trajectory of a ball inside the reactor is shown in the vertical projection in the top right position.

centrifugal forces generated by the synchronous rotations give rise to a net force that undergoes a periodic variation during the mill working cycle. Within a wide interval of rotation speeds, such force first makes the ball roll on the reactor wall, then pushes it across the reactor chamber, and finally determines its collision with the reactor wall. Figure 2 also shows the typical ball trajectory inside the moving reactor.

DOI: 10.1021/acsomega.8b01431
ACS Omega 2018, 3, 9196−9209

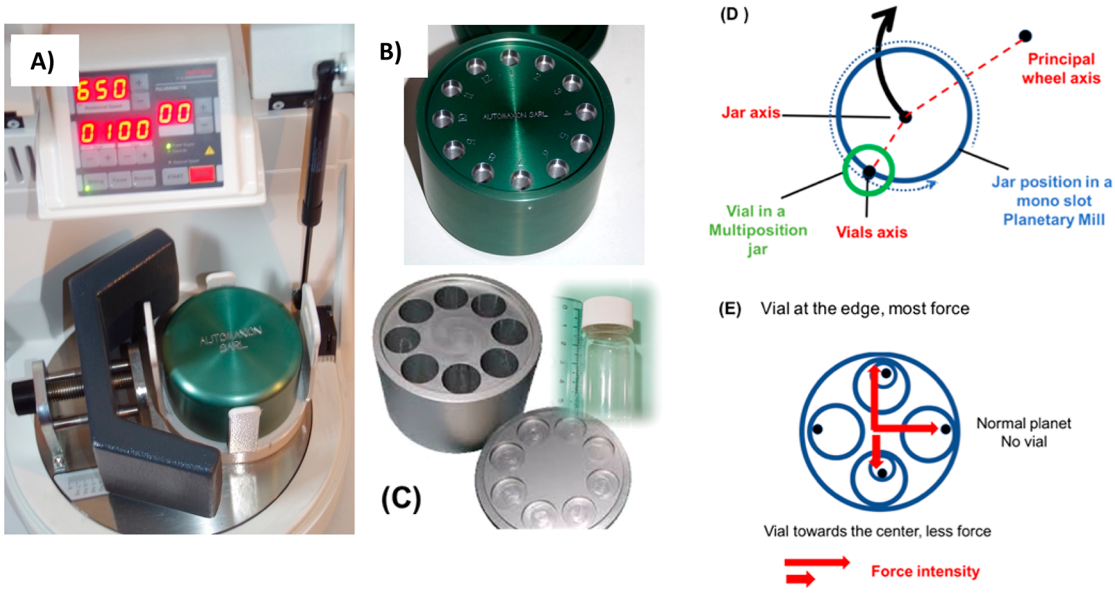

Figure 3. (A) A multisample planetary mill. (B) A 12-position jar hosting 2 mL GC/LC glass vials. (C) An 8-position jar hosting 20 mL glass vials. (D) Schematic description of the "lunar movement". (E) Variation of force intensity depending on the vial position. Panels C–E reproduced with permission from ref 52. Copyright 2013 The Royal Society of Chemistry.

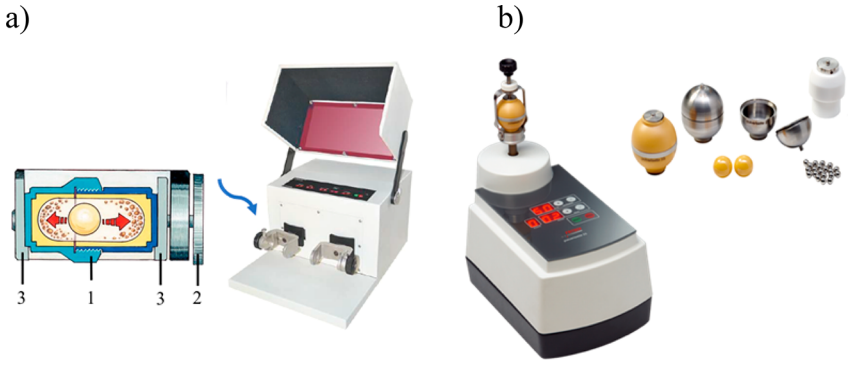

Figure 4. (a) Schematic cross-section of the round-ended, horizontally oscillating vial consisting of (1) jar body, (2) screw-on cap, and (3) holding clamps for FormTechSci Mill FTS1000 (image reproduced by kind permission from FormTechSci, Canada). (b) Fritsch Mini-Mill Pulverisette 23 and available bowls and balls (image reproduced by kind permission from Fritsch France).

Fritsch GmbH and Retsch GmbH produce the most popular planetary ball mills. The Fritsch Pulverisette P5 and P6 models are equipped with vials and balls made of different materials and cover capacities between 12 and 500 mL. High-speed planetary ball mills were manufactured to reach rotational speeds up to 1100 rpm, which result in centrifugal accelerations up to almost 100 times Earth's gravity.

The milling dynamics of planetary mills is also susceptible to characterization using the experimental method developed for the SPEX Mixer/Mill 8000. However, no attempt has been made in such direction to date. Thus, most available information comes from numerical simulations and strictly phenomenological empirical evidence. Numerical simulations suggest that the amount of mechanical energy that can be transferred to the powder during a collision depends on the velocity of the ball and on the angle of contact between the colliding milling media.[18,21−24,26,27,44] Indirect evidence has been noted from the study of physical and chemical transformations that point out that the transformation rate, and the nature of transformation itself, depend on the milling frequency and the mass and number of balls, thus indicating a role of collision energy.[18,21−24,26,27,44] Numerous studies have been performed to estimate such quantities from the numerical description of the milling dynamics.[28,36,37,40] To such aim, different combinations of milling parameters, including ball number and size, powder charge, and rotation speeds of disk and reactor, have been considered.[31,34,35] Numerical findings suggest that individual balls typically collide with energy between 0.01 and 0.65 J, and that collisions involving energies between 0.50 and 0.65 J occur at a frequency between 12 and 30 Hz, depending on the processing conditions. Correspondingly, the specific power dissipated during collisions can span the interval from approximately 2.5 to 22.5 J g^{-1} s^{-1}.[31,34,35,38,39]

The Uni-Ball Mill, which mainly finds application in the preparation of nanostructured materials and alloys, also deserves mention.[45,46] In the Uni-Ball Mill, the ball motion is confined to the vertical plane and is controlled by the configuration of external permanent magnets. This setup allows the coexistence of shearing and impact operation modes. The impact velocity can reach to 1.5 m s^{-1}. Collision frequency in the impact mode ranges from 1 to 2 Hz. Calculations based on Hertz impact theory suggest maximum impact stress of 37 kbar.[45]

DOI: 10.1021/acsomega.8b01431
ACS Omega 2018, 3, 9196−9209

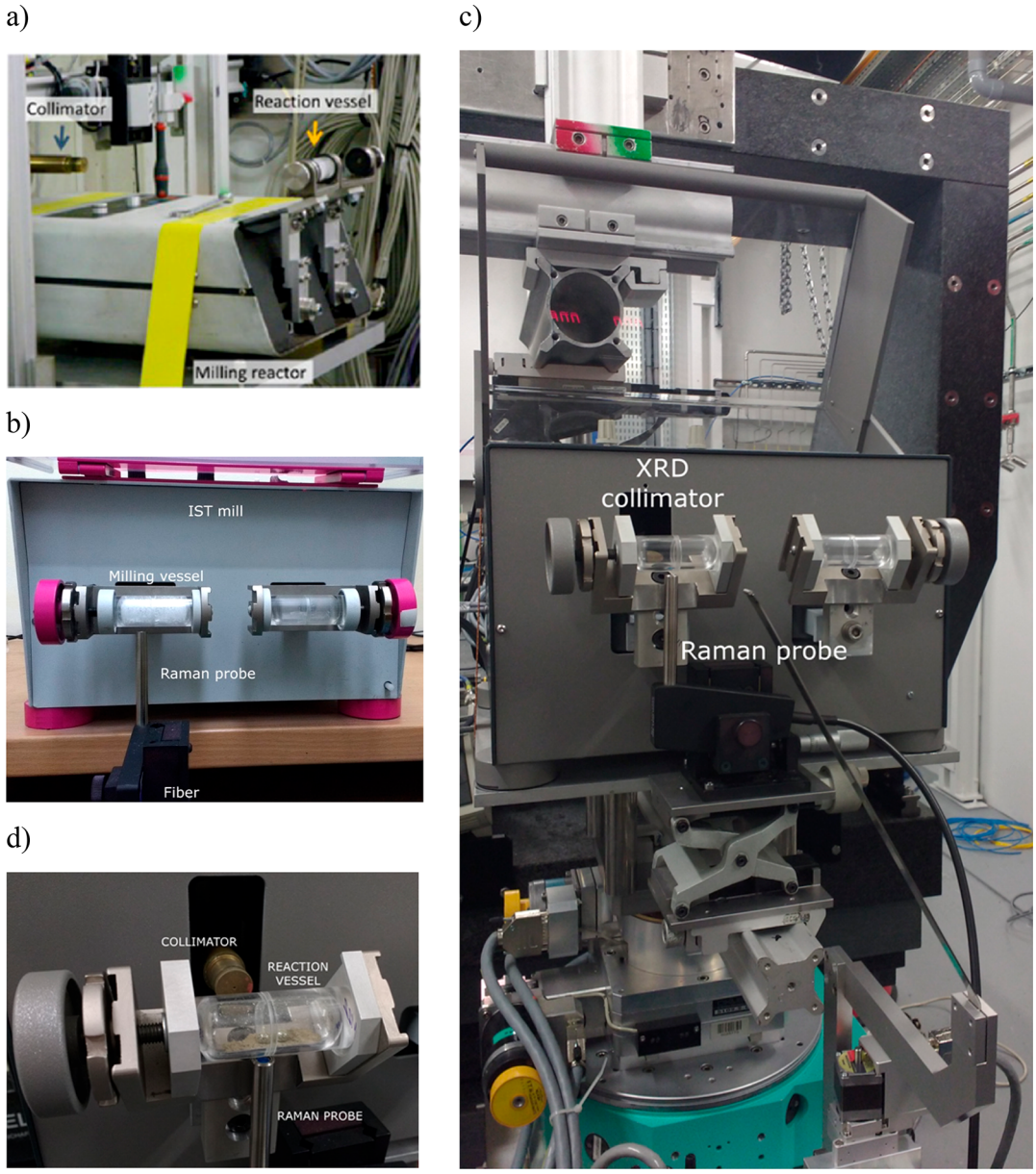

Figure 5. Experimental setup for collecting data *in situ* during mechanical processing through (a) synchrotron X-ray diffraction, (b) Raman spectroscopy, and (c) Raman spectroscopy and X-ray diffraction in tandem. (d) Magnification of transparent poly(methyl methacrylate) vial containing two 10 mm stainless steel balls. Panel a is reproduced with permission from *J. Phys. Chem. Lett.* **2015**, *6*, 4129−4140. Copyright 2015 American Chemical Society. Panels b−d are reproduced by kind permission from In Solido Technologies, Croatia.

For other ball mills, essentially no information is available. Therefore, it would be highly desirable to deepen the insight into their milling dynamics in the light of the usefulness of such devices for preparing chemicals and materials as well as for monitoring mechanically activated transformations.

This is the case, for instance, of the recently developed planetary milling system shown in Figure 3, which has been developed by Automaxion SARL. It uses adapters to hold multiple vials instead of normal jars, thus allowing the simultaneous processing of various samples. It has also been used to reduce the particle size of diverse materials down to 0.1 μm, to disperse pigments for inks and coatings,[47] and to screen co-crystals for minimal quantities of drugs.[48,49] It has also been utilized for the "parallel synthesis" of 3,4-dihydro-2*H*-benzo-[*e*][1,3]oxazine derivatives, thus showing the convenience of processing simultaneously up to 48 samples.[50]

The eccentric position of vials and the combined rotation of jar and support disk, evident from Figure 3D, impart the milling ball a net force different from the one typically experienced by balls in a conventional planetary mill, depicted in Figure 3E. Therefore, characterizing the milling dynamics is of primary importance for the suitable control of experimental conditions.[50,51]

Analogous considerations hold for the Retsch MM200 and MM400 Mixer Mills, which can work with 2−50 mL samples at frequencies between 3 and 30 Hz, and the compact benchtop mill FTS1000 released by FormTechSci, with a comparable range of grinding frequency and a mechanical action described in Figure 4a. Such operational features allow, depending on the powder charge, a variation of the impact velocity of milling balls against the reactor walls approximately between 0.1 and 7 m s^{-1}, with collision frequencies as high as

DOI: 10.1021/acsomega.8b01431
ACS Omega 2018, 3, 9196−9209

60 Hz. Similarly, characterization of milling dynamics is highly desirable for the Fritsch Mini-Mill Pulverisette 23 shown in Figure 4b, which imparts a spherical grinding bowl containing 0.1−5 mL samples vertical oscillations at frequencies between 15 and 50 Hz.

The need of a complete characterization of milling conditions appears even more urgent in the case of the milling equipment dedicated to the *in situ* monitoring of mechanically activated transformations (Figure 5) using synchrotron X-ray diffraction[52] and time-resolved Raman spectroscopy,[53] also in tandem.[54]

A modified Retsch Mixer mill MM200, shown in Figure 5a, was used for the quantitative *in situ* powder X-ray diffraction analysis of a mechanochemical process.[52,55] Later on, In Solido Technologies manufactured the mixer mill IST600 shown in Figure 5b. It is equipped with a plug-and-play *in situ* monitoring system, evident from Figure 5c, enabling synchrotron X-ray diffraction and Raman spectroscopy. Allocating up to four jars with a volume between 1 and 250 mL, the mill works at frequencies ranging between 3 and 33 Hz. When equipped with a ThermoJar system, the *in situ* measurement of local temperatures under milling conditions is also possible. Very recently, a new experimental setup for the study of milling reactions in real-time was released. It consists of an *in situ* triple coupling associating the simultaneous recording of X-ray diffraction patterns, Raman spectra, and thermograms to correlate structural evolution with temperature information during milling.[56]

3. KINETIC MODELING

The availability of detailed information on the relationship between milling dynamics and the nature and rate of physical and chemical transformations, and the real-time *in situ* measurement of physical properties, show the promise of leading mechanochemistry to a crucial turning point.[4,27,57−61] In particular, the enhanced accuracy in evaluating transformation kinetics can be expected to facilitate progress connected with the fundamental aspects of mechanical activation. In fact, it can give considerable help in the development of kinetic models aimed at linking empirical observation to local microscopic processes taking place during individual collisions.

In this respect, a relatively simple, phenomenological modeling approach can be derived starting from the fundamental features of the mechanical processing by BM. This latter is characterized by the continual stirring of the powder charge, which then keeps a high degree of chemical uniformity during the entire mechanical processing. The trapping of powder between the colliding milling media is approximately stochastic, and only a small volume V^* of the trapped powder is effectively processed during each collision, i.e., subjected to critical loading conditions (CLCs) severe enough to activate a given transformation. It follows that the powder charge can be divided into volume fractions $k = V^*/V$, where V is the total volume of powder, which have the same probability of being effectively processed during a collision.

As discussed in detail in our previous study,[62] statistical analysis of the BM process indicates that, for $k \ll 1$, the variation of the volume fractions of powder effectively processed 0 and i times, with the number of collisions n, is approximately described by the expressions

$$\chi_0(n) = e^{-kn} \tag{1}$$

$$\chi_i(n) = \frac{(kn)^i}{i!} e^{-kn} \tag{2}$$

which satisfy the mass balance condition $\sum_{i=0}^{\infty} \chi_i(n) = 1$.

Equations 1 and 2 can be used to describe the kinetics of mechanically induced transformations. For instance, the mass fraction of material transformed can be expressed as

$$\chi_{transf}(n) = 1 - e^{-kn} \tag{3}$$

under the hypothesis that transformation already occurs when the material is subjected to CLCs once, and further involvement in collisions has no consequence. Along the same line, if the material transforms only after two CLCs, the mass fraction of material transformed can be expressed as

$$\chi_{transf}(n) = 1 - (1 + kn) e^{-kn} \tag{4}$$

The model is quite versatile and allows the definition of a set of equations able, in principle, to best fit experimental kinetic curves.

Similarly, eqs 1 and 2 can also be used to describe the microstructural evolution of a given phase. For instance, it can be assumed that the powder fraction subjected to i CLCs has average crystallite size L_i. Therefore, the average crystallite size L that can be obtained by averaging over the total powder charge is equal to

$$L = \sum_{i=0}^{n} \chi_i(n) L_i = \left[L_0 + KnL_1 + \frac{(Kn^2)}{2} L_2 + \ldots \right] e^{-kn} \tag{5}$$

where L_0, L_1, L_2, ... L_i are the average crystallite sizes of the powder fractions that have undergone CLCs 0, 1, 2, ... i times, respectively. Quite often, experimental evidence indicates that the crystallite size of any given fraction of powder submitted to CLCs drops from the initial L_0 value to the final L_f one after a single CLC event. Under such circumstances, $L_0 \neq L_1 = L_2 \ldots = L_i \ldots = L_f$, and eq 5 can be rewritten as

$$L = L_0 e^{-kn} + L_f(1 - e^{-kn}) \tag{6}$$

Similar expressions can be written starting from eq 5 and specializing L_i values.

According to eqs 1−6, the rate of a mechanically activated transformation depends on the quantity k. The larger its value, the faster the transformation is. Therefore, k can be regarded as the apparent rate constant of the transformation. Since mechanically activated transformations do not necessarily involve chemical reaction, k does not necessarily correspond to rate constants typically defined in chemical kinetics. Nevertheless, it can be considered a chemical rate constant whenever the mechanically activated transformation involves a chemical reaction.

In its broadest definition, k measures the volume V^* of powder where the mechanically activated transformation occurs. The volume V^* is not a *continuum*. Instead, it is the sum of smaller volumes that can be thought to be irregularly distributed within the volume of powder subjected to mechanical loading during individual collisions. In turn, such smaller volumes can be regarded as the volumes within which the local mechanical stresses generated during the collision induce the transformation.

Therefore, k represents merely an estimate of the amount of pristine material involved in the mechanically activated transformation. Since no information is available on the

DOI: 10.1021/acsomega.8b01431
ACS Omega 2018, 3, 9196−9209

mechanism governing the transformation, and no assumption is made in such regard, it cannot be excluded that the overall rate of transformation depends on two or more stages. Therefore, following in this classical chemical kinetics, it is more appropriate to look at k as an apparent rate constant.

Although the model is phenomenological, and therefore k is a phenomenological constant, a better understanding of its physical meaning is strictly necessary to foster further progress in the modeling description of the transformation kinetics. In this respect, existing literature focusing on the development of a kinetic approach for mechanochemical transformations based on non-equilibrium thermodynamics can be quite useful.[63] However, significant work must be still performed to allow the coherent development of a conceptual framework for providing a rigorous interpretation of the thermodynamic and kinetic features connected with the rate constant of mechanically activated processes. Hopefully, this specific subject will become an active and popular area of research.

All the model equations developed heretofore hold validity if expressed as a function of time, t. Time and number of collisions are related by the product $n = Nt$, where N is the frequency of collisions. Therefore, $kn = kNt = Kt$, where $K = kN$ is the apparent rate constant referred to the time scale. K expresses merely the volume of powder subjected to CLCs per unit time.

In the following, a few specific examples will be discussed to show the capability of the model for interpolating experimental points.

4. RESULTS AND DISCUSSION

4.1. Kinetic Evidence. Literature is relatively lacking in reports including experimental curves describing transformation kinetics quantitatively. Despite the considerable attention devoted in the past to mechanical activation, only in a few cases have the formation of inorganic phases from a set of reactants, the phase transition from one polymorph to the other, and the reaction between two or more chemicals been satisfactorily investigated in this respect. In most cases, only qualitative and indirect kinetic and mechanistic inferences have been gathered starting from empirical observation.

The kinetic analysis of refined experimental data sets, even with a simple kinetic model such as the one described above, can provide interesting information on the way mechanical activation by BM works. A few case studies, spanning from individual metals to mixtures of organic compounds, are discussed.

4.1.1. Formation of Nanostructures. Mechanical activation has been extensively used to induce the reduction of grain size, L, in pristine crystalline materials. For some metals, minerals, and ceramics processed individually and in the mixture, L varies with the number of collisions, n, as can be seen in Figure 6. It undergoes a smooth monotonic decrease from an initial value, L_0, to a final asymptotic one, L_f. L_0 is not a meaningful quantity, being mostly determined by the process employed to produce the commercial powders. Conversely, L_f depends on both material properties and processing conditions.[64]

As evident from Figure 6, eq 6 satisfactorily reproduces the experimental behavior. This suggests that the assumptions underlying the mathematical expression, namely the fact that the grain size in a volume subjected to CLCs once changes discontinuously from the initial value, L_0, to the final one, L_f, can represent a physical situation. According to the best fitting, the apparent rate constant, k, is approximately equal to 3.2×10^{-6}. Based on the model interpretation of k, this value expresses the ratio V^*/V between the volume V^* of trapped powder effectively processed during each collision and the total volume V of powder. If the density of effectively processed powder does not differ from that of the pristine powder, k is also equal to m^*/m. Here, m^* is the mass of powder effectively processed during each collision, and m is the total mass of powder inside the reactor. Since the data shown in Figure 6 were obtained from experiments using a total mass of Cu of 8 g, the amount of powder effectively processed during any individual collision, i.e., subjected to a decrease of the grain size consequent to the mechanical stresses generated by the colliding milling tools, is equal to about 24 μg.

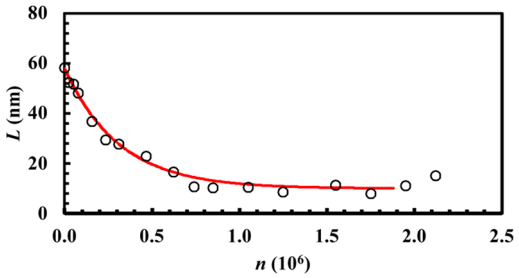

Figure 6. Average crystallite size L of Cu as a function of the number of collisions, n. The best-fitted curve is also shown.

4.1.2. Reactivity of Solids. Previous work has shown that BM induces the formation of radical species at the surface of quartz powder subjected to BM.[65] Radical generation was monitored using the 2,2-diphenyl-1-picrylhydrazyl (DPPH) in ethanol solution as radical scavenger.[65] UV−vis spectrophotometric analyses indicate a consumption of DPPH due to the interaction of DPPH with the hydrogen radicals, $H^\bullet$, formed in solution by reaction of the C_2H_5OH molecules with the silyl, $\equiv Si^\bullet$, and siloxyl, $\equiv Si-O^\bullet$, radicals at the surface of quartz powders. The reaction scheme can be summarized as indicated below:[65]

$$\equiv Si-O-Si\equiv \rightarrow \equiv Si^\bullet + \equiv Si-O^\bullet \quad (a)$$

$$\equiv Si^\bullet + C_2H_5OH \rightarrow \equiv Si-OC_2H_5 + H^\bullet \quad (b)$$

$$\equiv Si-O^\bullet + C_2H_5OH \rightarrow \equiv Si-OH + {}^\bullet C_2H_4OH \quad (c)$$

$$DPPH + H^\bullet \rightarrow DPPH\text{-}H \quad (d)$$

The mechanical activation first determines the formation of surface radicals $\equiv Si^\bullet$ and $\equiv Si-O^\bullet$. The radicals then react with ethanol molecules to form $H^\bullet$. Finally, $H^\bullet$ combines with the DPPH to form neutralized DPPH-H.

The number N_{DPPH} of moles of DPPH in ethanol solution is shown in Figure 7a as a function of the number of collisions, n, undergone by quartz. N_{DPPH} decreases smoothly at a rate that becomes increasingly lower as n increases. After about 2×10^6 collisions, the N_{DPPH} decrease becomes linear.

The N_{DPPH} data in Figure 7a can be related to the values of the average specific surface area S of quartz powders, which are shown in Figure 7b.

The surface area S shown in Figure 7b can be satisfactorily described by the mathematical expression

$$S = S_{in}\, e^{-kn} + S_{fin}(1 - e^{-kn}) \quad (7)$$

where k is the apparent rate constant for the surface area increase and S_{in} and S_{fin} are the initial and final S values, respectively. Such expression is similar to eq 5 and suggests

DOI: 10.1021/acsomega.8b01431
ACS Omega 2018, 3, 9196−9209

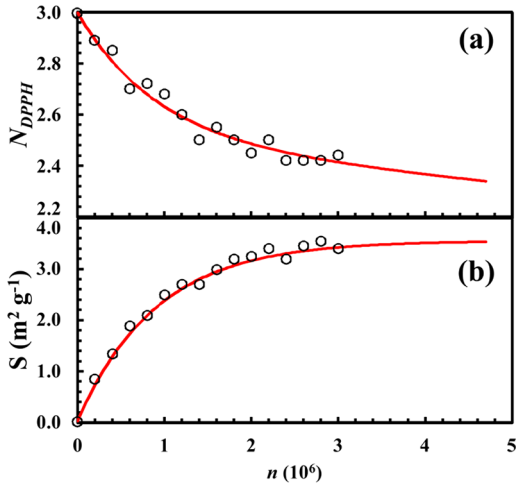

Figure 7. (a) Number of moles of DPPH in ethanol solution, N_{DPPH}, and (b) average specific surface area of quartz powders, S, as a function of the number of collisions, n. Best-fitted curves are also shown.

that S can be regarded as the weighted average of the surface areas S_{in} and S_{fin} exhibited by the fractions of quartz powders e^{-kn} and $1 - e^{-kn}$. Thus, e^{-kn} measures the fraction of quartz powders that retains the initial specific surface area S_{in}, whereas $1 - e^{-kn}$ is the fraction that has reached the final specific surface area S_{fin}. Accordingly, any given collision makes a certain amount of quartz powders change abruptly its average specific surface area from S_{in} to S_{fin}. The rate constant k is approximately equal to 1.1×10^{-3}. The total mass of powder subjected to processing being equal to 2 g, the mass of quartz powders effectively involved in collisions corresponds to about 2.2 mg.[65]

Two different kinds of active sites can be thought to coexist at the surface, namely those generated by fracture of quartz particles involved in a collision, which increases the specific surface area S, and those generated by attrition between quartz particles, which does not lead to a change of S. The active sites formed by fracture or by attrition can have different chemical activities. If N_f and N_a are the numbers of active sites formed, respectively, by fracture and attrition, the DPPH consumption can be described by the expression

$$-dN_{DPPH} = (N_f + N_a)\, dn \tag{8}$$

N_f and N_a are proportional, respectively, to the surface area generated by fracture at individual collisions and to the total surface area of powder particles involved in individual collisions. The increase of specific surface area as a function of the number of collisions can be obtained by differentiating eq 7, whereas the surface area generated by fracture can be obtained by multiplying the specific surface area increase by the mass m_p of powder charge. Therefore, N_f and N_a can be expressed as

$$N_f = \alpha k m_p (S_{fin} - S_{in})\, e^{-kn} \tag{9}$$

and

$$N_a = \beta k m_p S \tag{10}$$

where α and β are proportionality constants. Based on eqs 9 and 10, the solution of eq 8 is

$$N_{DPPH} - N_{DPPH,in} = -m_p[\beta k S_{fin} n + (\alpha - \beta)(S_{fin} - S_{in})(1 - e^{-kn})] \tag{11}$$

where $N_{DPPH,in}$ is the initial number of moles of DPPH.

Equation 11 interpolates the experimental N_{DPPH} data shown in Figure 7a quite well, providing best-fitted values for α and β equal to about 8.1×10^{-5} and 4.7×10^{-6} mol m^{-2}, respectively. These numbers provide a quantitative estimate of the surface density of active sites generated by fracture or attrition, respectively. A comparison with the maximum possible number of dangling bonds that can be formed at the surface, equal to about 2.1×10^{-5} mol m^{-2}, clearly shows the high level of structural excitation attained by mechanically activated quartz surfaces.

4.2. Formation of Crystalline Solid Solutions. The mutual dissolution of Ag and Cu represents a typical example of mechanical alloying.[66] Despite the immiscibility of the two elements, due to a relatively high positive enthalpy of mixing, BM induces the formation of a crystalline, chemically disordered, homogeneous solid solution.

The formation of the solid solution follows relatively complex kinetics. The dissolution of Ag atoms into the Cu matrix forms a Cu-rich solid solution, hereafter indicated as Cu(Ag). At the same time, the dissolution of Cu atoms into the Ag matrix forms an Ag-rich solid solution, hereafter indicated as Ag(Cu). A third solid solution, hereafter indicated as (AgCu), forms as a result of the combination of the two Ag(Cu) and Cu(Ag) solid solutions, which can be then regarded as intermediates.

The mass fractions χ of Cu in the different phases are shown in Figure 8 as a function of the number of collisions, n. Initially,

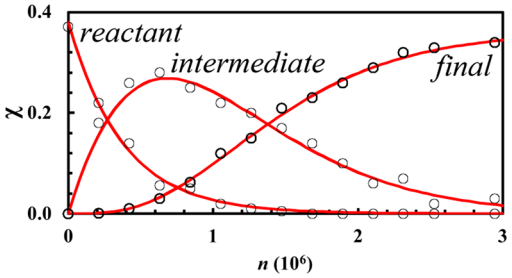

Figure 8. Mass fraction, χ, of Cu involved in reactant, intermediate, and final phases as a function of the number of collisions, n. Best-fitted curves are also shown.

the mass fraction of reactant Cu, χ_{reac}, corresponds to the mass fraction of Cu in the mixture, $\chi_{Cu,0}$. For simplicity, the mass fractions of Cu in Ag(Cu) and Cu(Ag) solid solutions are summed to give the total mass fraction of Cu in intermediate phases, χ_{int}. The mass fraction of Cu in the final product, χ_{fin}, consists of the mass fraction of Cu in the final (AgCu) solid solution. Whereas χ_{reac} undergoes a smooth decrease, χ_{int} exhibits a maximum, and χ_{fin} follows an increasing sigmoidal trend.

Starting from eqs 1 and 2, the kinetic model provides suitable expressions for describing the kinetic evolution of Cu in reactants, intermediates, and products.[66] The consumption of reactant Cu is described by the equation

$$\chi_{reac} = \chi_{Cu,0}\, e^{-kn} \tag{12}$$

DOI: 10.1021/acsomega.8b01431
ACS Omega 2018, 3, 9196−9209

where $\chi_{Cu,0}$ is the initial amount of Cu in the $Ag_{50}Cu_{50}$ powder mixture. The kinetics of Cu in intermediates is described by

$$\chi_{int} = \chi_{Cu,0}\left[kn + \frac{(kn)^2}{2} + \frac{(kn)^3}{6}\right] e^{-kn} \quad (13)$$

whereas the fraction of Cu in the final product is accounted for by the expression

$$\chi_{fin} = \chi_{Cu,0}\left\{1 - \left[1 + kn + \frac{(kn)^2}{2} + \frac{(kn)^3}{6}\right] e^{-kn}\right\} \quad (14)$$

It follows that Cu becomes involved in the formation of the intermediate Ag(Cu) and Cu(Ag) solid solutions already after the first collisions, and that the intermediates transform into the final (AgCu) solid solution after the third collision. It appears that the whole sequence of transformations can be described satisfactorily using a single rate constant, k. Best fitting suggests a k value of about 2.2×10^{-6}. Since experiments were performed using a total mass of Cu equal to 8 g, the amount of powder effectively processed during any individual collision is approximately equal to 17 μg.

4.3. Formation of Amorphous Alloys. The mechanical processing of $Ni_{40}Ti_{60}$ powder mixtures by BM induces the formation of an amorphous phase.[67] A representative kinetic curve is shown in Figure 9. With the sigmoidal conversion to the amorphous phase obtained for collision energy of about 0.10 J, a satisfactory best fit can be obtained using eq 4.

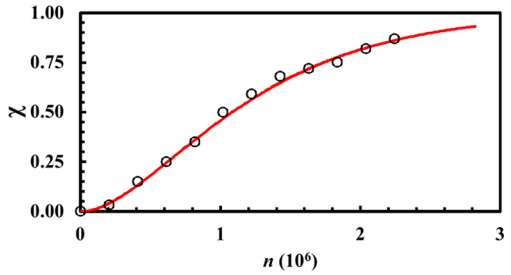

Figure 9. Mass fraction of amorphous phase, χ, as a function of the number of collisions, n. The best-fitted curve is also shown.

According to the assumptions employed to develop the kinetic model, the results mentioned above indicate that amorphization takes place in fractions of $Ni_{40}Ti_{60}$ powders that have undergone at least two CLCs.

The apparent rate constant, k, for the amorphization process is approximately equal to 1.5×10^{-6}. The experiments were performed with a total mass of powder of 8 g. Therefore, the amount of powder effectively processed at collision is equal to about 12 μg.

4.4. Formation of Co-crystals. The mechanical processing by BM allows mixing two or more chemicals on the molecular scale, resulting in the formation of co-crystals.[68−70] For instance, clear kinetic evidence has been obtained in the binary nicotinamide−benzoic acid (na:ba) system using quantitative *in situ* monitoring by tandem X-ray diffraction and Raman spectroscopy.[70] The data referring to the liquid-assisted grinding of a stoichiometric na:ba powder mixture in the presence of 4.1 mL of methanol are shown in Figure 10.

Mechanical processing in the presence of methanol leads to the formation of polymorph II co-crystal, the process being complete within approximately 6 min. Further mechanical treatment up to 3 h does not induce modifications. Under the assumption that a linear relationship between the number of collisions, n, and the time, t, exists, the model equation

$$\chi_{fin} = 1 - (1 + Kt)\, e^{-Kt} \quad (15)$$

can be written. It is able to best fit satisfactorily the experimental points, suggesting for the apparent rate constant K value of about 0.13 min^{-1}. Accordingly, about the 13% of the volume of powder is effectively processed per minute of mechanical treatment.

4.5. Formation of MOFs. *In situ* measurements have also been used to monitor the mechanochemical synthesis of zeolitic MOF ZIF-8 from 2-methylimidazole and ZnO.[52] The mechanical processing by BM induces a gradual modification of X-ray diffraction patterns. As shown in Figure 11, the strongest reflection for ZIF-8 varies according to a sigmoidal trend.

An expression similar to eq 15 can be written to interpolate the experimental points as a function of time, t. Specifically, the variation of the relative intensity of the (211) reflection belonging to the X-ray diffraction pattern of the ZIF-8 final product can be described using the expression

$$I = I_{fin}[1 - (1 + Kt)\, e^{-Kt}] \quad (16)$$

where I_{fin} represents the final value of the relative intensity and K is the apparent rate constant for the intensity variation. The above equation can interpolate satisfactorily the experimental data set with an apparent rate constant K of about 0.25 min^{-1}.

4.6. Synthesis of Organic Compounds. Mechanical activation by BM has also been successfully used to the preparation of organic compounds. *In situ* Raman analyses have been performed to monitor the mechanochemical

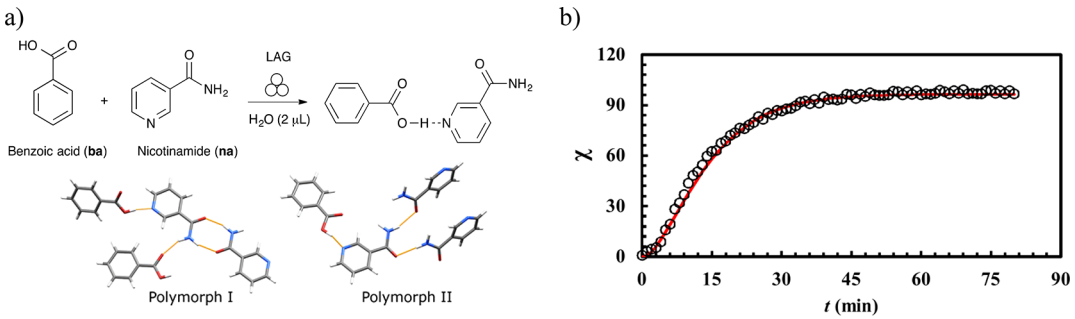

Figure 10. (a) Some of the polymorphs obtained from benzoic acid and nicotinamide (na:ba 1/1) by liquid assisted grinding (LAG) with water. (b) Mass fractions of the polymorph II na:ba co-crystal as a function of time, t. Best-fitted curves are also shown.

DOI: 10.1021/acsomega.8b01431
ACS Omega 2018, 3, 9196−9209

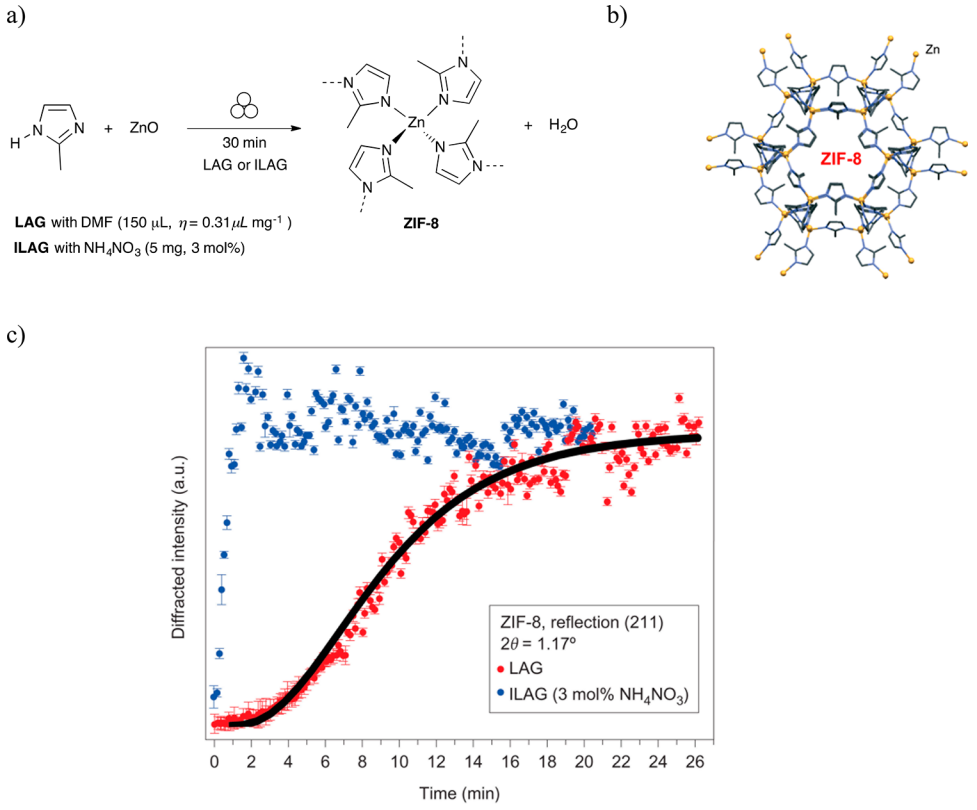

Figure 11. (a) Mechanosynthesis of ZIF-8 from 2-methylimidazole (HMeIm) and ZnO. (b) Part of the crystal structure of ZIF-8. (c) Relative intensity of the (211) reflection of the X-ray diffraction pattern of the ZIF-8 final product (ILAG = ion liquid assisted grinding). The best-fitted curve is also shown. Panels b and c are adapted from ref 52 with permission from Springer.

Scheme 1. Preparation of 2,3-Diphenylquinaxoline by Neat Milling[71]

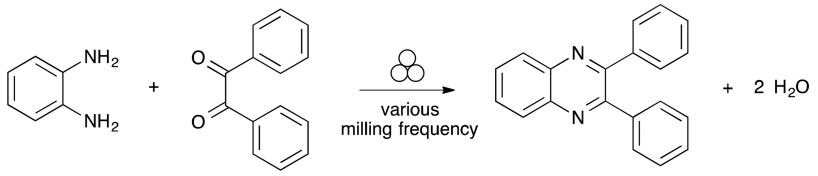

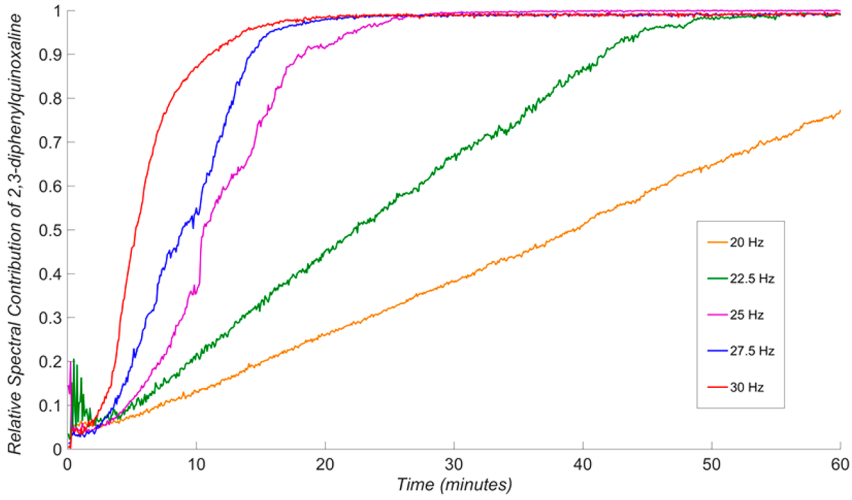

Figure 12. Effects of milling frequency on the kinetic behavior of a condensation reaction. Reproduced with permission from ref 71. Copyright 2017 Julien et al. (http://creativecommons.org/licenses/by/4.0).

condensation between benzyl and *o*-phenylenediamine described in Scheme 1.[71] The experimental curves shown in Figure 12 reveal a remarkable dependence of reaction rate on the BM frequency. Such dependence has been tentatively

DOI: 10.1021/acsomega.8b01431
ACS Omega 2018, 3, 9196−9209

Scheme 2. Mechanochemical Condensation of Barbituric Acid and Vanillin (Knoevenagel Reaction)

explained invoking different mechanical activation regimes at low and high milling frequencies, essentially due to the differences in the mechanical energy transferred to powders when frictional or impulsive processes prevail.

Concerning the mechanochemical organic synthesis, it is worth noting that not all of the data available can be subjected to satisfactory interpolation by the model equations. For instance, this is the case of the Knoevenagel condensation reaction between vanillin and barbituric acid, described in Scheme 2, and with data summarized in Figure 13.[72] It displays an exponential kinetic curve in solution, while sigmoidal kinetics has been demonstrated under BM conditions by *ex situ* analyses.

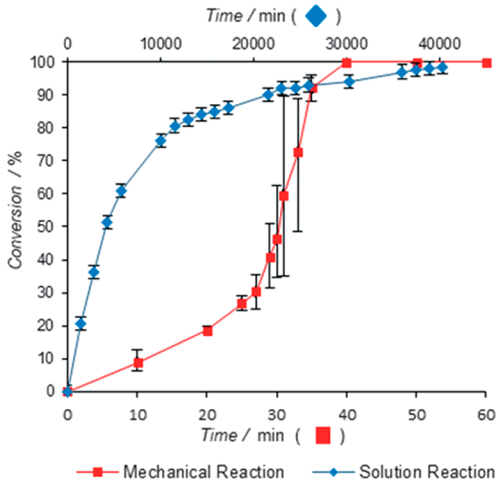

Figure 13. Kinetic profiles for the Knoevenagel condensation reaction in solution or under mechanical processing conditions. Reproduced with permission from ref 72. Copyright 2017 Wiley-VCH Verlag GmbH & Co. KGaA.

The reaction kinetics was independent of both the amount of water inside the jar and the particle size of reactants. Nonetheless, the reaction rate increased changing the milling frequency from 15 to 30 Hz and decreased when the reaction scale passed from 0.25 to 1 g. Interestingly, milling induces the transformation of the initial granular body into a sticky material that adheres to the ball almost uniformly, giving rise to a homogeneous coating.[73] The formation of such coating definitely affects the milling dynamics, probably leading to the rate enhancement of the reaction, and points out how changes in rheological properties of processed matter can give rise to kinetic effects out of reach for purely physicochemical models.

Sigmoidal kinetic profiles, obtained by *ex situ* analyses, were observed during the formation of 1-(4-chlorophenyl)-2-(2-nitrophenyl)disulfane heterodimer. Depending on the experimental milling conditions, achieved neat or adding acetonitrile, different polymorphs were formed as indicated in Scheme 3.[74]

The *in situ* investigation of kinetic behavior allows attaining unprecedented detail on the transformation path, unveiling short-lived intermediates and disclosing minute aspects of experimental evidence. All of that bears the great promise of deeply impacting the field, catalyzing progress in the definition of kinetic schemes and the description of macroscopic differential and integral kinetic laws involved in mechanically induced processes.

5. MECHANISTIC INFERENCES

Coupled with the time-resolved investigation, *in situ* observation can be also exploited to gain information on mechanistic issues. In particular, examining the response of the material to impulsive loading can allow obtaining mechanistic evidence on the effects of mechanical stresses on the molecular level.

Toward this aim, ball drop experiments offer an interesting opportunity. Indeed, it is relatively easy to combine them with experimental methods enabling the exploration of the time and length scales of local processes activated by individual collisions.

The preliminary data on mechanistic inferences have been obtained by performing luminescence measurements. The experiments were performed on thin layers of coumarin 1 powder deposited on a transparent alumina window. A steel ball of 10 mm in diameter was dropped from a selected height to collide with the powder layer at a velocity of 5 m s^{-1}, which is close to the collision velocities typically observed in SPEX Mixer/Mill 8000.

Scheme 3. Different Milling Conditions Determine Which Polymorph Is Formed

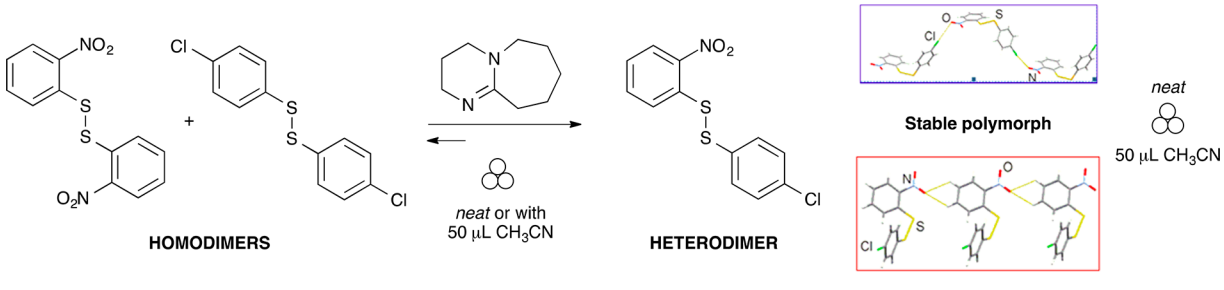

DOI: 10.1021/acsomega.8b01431
ACS Omega 2018, 3, 9196−9209

Coumarin 1 has a characteristic broad emission around the wavelength of 440 nm, with an excitation band in the near UV region. Coumarin 1 powder was continuously excited with a focalized laser beam and its luminescence was analyzed with an intensified CCD camera equipped with a Peltier thermoelectric cooling.

Excitation was provided by the 405 nm laser line and collected at 180° through the transparent alumina window by a fiber-coupled microscope. Spectrally resolved luminescence before, during and after collisions was monitored using a temporal gate below 10 ms. A picture of the zone affected by the ball drop, obtained using an optical microscope, is shown in Figure 14a. Relative luminesce recorded after the collision in steady time PL condition is shown in Figure 14b together with the emission of the pristine coumarin 1 for comparison.

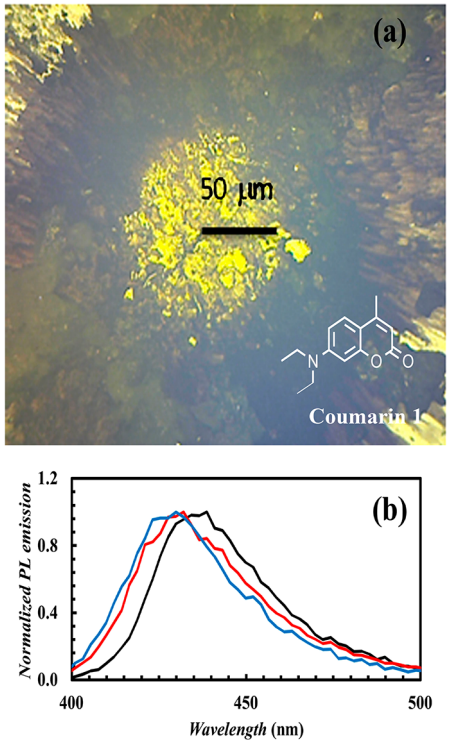

Figure 14. (a) Region of the coumarin 1 powder layer affected by the ball drop. (b) Photoluminescence sampled from initial coumarin 1 (black curve), and from the inner (blue curve) and outer (red curve) zones of the region affected by the ball drop.

Luminescence measurements show that the coumarin 1 located in the region affected by ball drop exhibits a blue shift with respect to the pristine powder. The shift observed was up to 20 nm in the inner zone of the region and progressively decreased with the distance from the center.[75] Collision effects were not reversible and were confined to an area less than 10 mm^2.

The Raman spectra collected from the pristine sample and the coumarin 1 region affected by ball drop are shown in Figure 15. They reveal that the irreversible changes in luminescence spectra induced by collisions cannot be ascribed to a variation of molecular structure, which remains unaffected.

Kinetics of luminescence during collisions was reconstructed collecting emitted radiation from the inner zone of the region affected by ball drop using temporal windows of 10 ms. The obtained spectra are shown in Figure 16. The spectroscopic

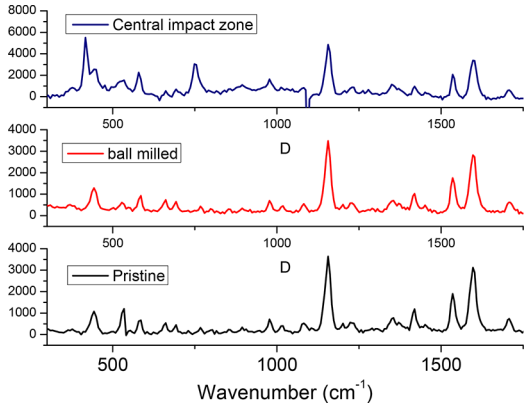

Figure 15. Raman spectra collected from (black curve) pristine coumarin 1 and from samples subjected to (blue curve) ball drop and (red curve) BM.

evidence points out that the blue shift takes place irreversibly on a time scale of about 30 ms.

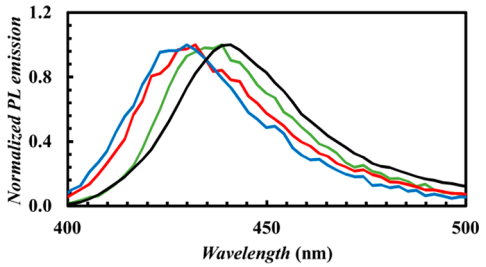

Figure 16. Photoluminescence sampled from the inner zone of the region affected by ball drop. Curves refer to coumarin 1 at the beginning of the ball collision (black curve) and after 10 (green curve), 20 (red curve), and 30 (blue curve) ms.

The obtained experimental findings can be connected with the fact that fluorescence in coumarin 1 is mainly due to its monomeric form. In particular, decay kinetics is related to the conversion of fluorescent intramolecular charge transfer (ICT) states to non-fluorescent twisted intramolecular charge transfer (TICT) related phenomena.[76] Within this framework, local effects caused by individual collisions can be tentatively explained invoking the formation of stacked dyes and H-type aggregates, which involves the restriction of the ICT to TICT charge transfer mechanism. Therefore, the observed blue-shift in the luminescence spectra can be reasonably ascribed to the emission from H-type aggregates.[77] While a blue shift in the absorption spectra is a general feature for H-type aggregates, depending on the excitonic states involved, the emission spectra of such aggregates exhibit either a blue shift or a red shift. According to previous works,[76,77] in coumarin 1 the emission related to the formation of H-type aggregates is mainly due to higher excitonic states, and, hence, generating a blue shift of the overall emission. It follows that the measured luminescence spectra indicate a local rearrangement of coumarin 1 molecules in the region of the powder layer affected by ball drop, due to the formation of highly interacting aggregates due to the collision.

The measurement of time-resolved luminescence spectra provides a direct tool to follow *in situ* the effects of mechanical stresses generated in the powder layer during ball collisions. Deeper insight into the local processes governing the

DOI: 10.1021/acsomega.8b01431
ACS Omega 2018, 3, 9196−9209

rearrangement of coumarin 1 molecules can be gained by decreasing area and time scale of investigation. This can be expected to give access to information regarding the way the collision generates mechanical stresses within the granular body. In principle, this offers the unique opportunity of relating the phenomenological interpretation of transformation kinetics to refined mechanistic evidence, enabling the explanation of kinetic data on a fundamental basis.

6. CONCLUSIONS

The kinetics of mechanically activated transformations is a critical issue along the road to the fundamental understanding of mechanochemical processes and the rational design of effective mechanical processing methods and tools. The general strategy for taking on the kinetic challenge is relatively clear. It involves the development of methods for characterizing and controlling the milling dynamics, the collection of refined experimental data and their interpretation with the help of specific kinetic models, and the study of microscopic processes activated by individual collisions. In this respect, the present state of the art appears quite fragmentary and contradictory. The kinetic evidence is still scarce and barely connected with milling dynamics.

The use of *in situ* investigations and the availability of new processing tools show promise to promote progress in the field. The interpretation of refined kinetic data with a simple, phenomenological model provides valuable information on the amount of powder susceptible to effective processing during individual collisions. In turn, this provides a first link to the local processes activated by the mechanical stresses generated at the point of collision.

Combining time-resolved studies with *in situ* investigation allows the direct measurement of the effects of mechanical stresses on individual molecules. Thus, it can help to enlighten researchers on the way mechanical loads act at the molecular level.

The correct interpretation of experimental findings in the light of milling dynamics and the mechanistic study of mechanochemical transformations represent crucial objectives to achieve. We hope that the present work will stimulate progress in the field.

AUTHOR INFORMATION

Corresponding Authors

*E-mail: evelina.colacino@umontpellier.fr.
*E-mail: francesco.delogu@unica.it.

ORCID

Evelina Colacino: 0000-0002-1179-4913
Andrea Porcheddu: 0000-0001-7367-1102
Pier Carlo Ricci: 0000-0001-6191-4613

Notes

The authors declare no competing financial interest.

ACKNOWLEDGMENTS

This work has been supported by the University of Cagliari (Italy). The authors are grateful to Dr. Ivan Halasz (Ruđer Bošković Institute, Zagreb, Croatia) for sharing *in situ* monitoring experimental data. The authors are grateful to M. Walter Oliveira (Fritsch Gmbh, Germany; www.fritsch-france.fr/), Dr. Aleksandar Sabljic (In Solido Technologies, Zagreb, Croatia; www.insolidotech.com/), Dr. Christopher Nickels (FormTechSci, Canada; https://formtechscientific.com/), and Dr. Stephen Bysouth (Automaxion, SARL, Varenguebec, France; http://www.automaxionltd.com/) for providing some of the high-resolution pictures used in the article, for technical details shared about the equipment, and for fruitful discussions during the preparation of the manuscript. Authors are grateful to Dr. Amit Kumar for the final reading and editing of the manuscript in the light of his full professional proficiency in English, which greatly helped in improving its readability.

REFERENCES

(1) Sopicka-Lizer, M., Ed. *High-Energy Ball Milling. Mechanochemical Processing of Nanopowders*; Woodhead Publishing: Cambridge, UK, 2010.
(2) Delogu, F., Mulas, G., Eds. *Experimental and Theoretical Studies in Modern Mechanochemistry*; Transworld Research Network, Kerala, India, 2010.
(3) Baláž, P.; Achimovičová, M.; Baláž, M.; Billik, P.; Cherkezova-Zheleva, Z.; Criado, J. M.; Delogu, F.; Dutková, E.; Gaffet, E.; Gotor Martinéz, F. J.; Kumar, R.; Mitov, I.; Rojac, T.; Senna, M.; Streletskii, A.; Wieczorek-Ciurowa, K. Hallmarks of mechanochemistry: from nanoparticles to technology. *Chem. Soc. Rev.* **2013**, *42*, 7571−7637.
(4) Suryanarayana, C. Mechanical alloying and milling. *Prog. Mater. Sci.* **2001**, *46*, 1−184.
(5) Delogu, F.; Cocco, G. Crystallite size refinement in elemental species under mechanical processing conditions. *Mater. Sci. Eng., A* **2006**, *422*, 198−204.
(6) Delogu, F.; Cocco, G. The size refinement of Cu crystallites under mechanical processing conditions: a phenomenological modeling approach. *J. Mater. Sci.* **2007**, *42*, 4356−4363.
(7) Witkin, D. B.; Lavernia, E. J. Synthesis and mechanical behavior of nanostructured materials via cryomilling. *Prog. Mater. Sci.* **2006**, *51*, 1−60.
(8) Zhang, D. L. Processing of advanced materials using high-energy mechanical milling. *Prog. Mater. Sci.* **2004**, *49*, 537−560.
(9) *Ball Milling Towards Green Synthesis: Applications, Projects, Challenges*; Stolle, A., Ranu, B., Eds.; RSC Green Chemistry Series; The Royal Society of Chemistry: Cambridge, UK, 2015.
(10) *Mechanochemistry: From Functional Solids to Single Molecule*; The Royal Society of Chemistry: Cambridge, UK, 2014; Vol. *170*.
(11) Margetic, D.; Strukil, V. *Mechanochemical Organic Synthesis*; Elsevier: Amsterdam, The Netherlands, 2016.
(12) Daurio, D.; Nagapudi, K.; Li, L.; Quan, P.; Nunez, F.-A. Application of twin screw extrusion to the manufacture of cocrystals: scale-up of AMG 517−sorbic acid cocrystal production. *Faraday Discuss.* **2014**, *170*, 235−249.
(13) Dhumal, R.; Kelly, A.; Coates, P.; York, P.; Paradkar, A. Cocrystalization and simultaneous agglomeration using hot melt extrusion. *Pharm. Res.* **2010**, *27*, 2725−2733.
(14) Medina, C.; Daurio, D.; Nagapudi, K.; Alvarez-Nunez, F. Manufacture of pharmaceutical co-crystals using twin screw extrusion: a solvent-less and scalable process. *J. Pharm. Sci.* **2010**, *99*, 1693−1696.
(15) Crawford, D. E.; Miskimmin, C. K. G.; Albadarin, A. B.; Walker, G.; James, S. L. Organic synthesis by Twin Screw Extrusion (TSE): continuous, scalable and solvent-free. *Green Chem.* **2017**, *19*, 1507−1514.
(16) Levitas, V. I. Continuum Mechanical Fundamentals of Mechanochemistry. In *High Pressure Surface Science and Engineering*; Gogotsi, Y., Domnich, V., Eds.; Institute of Physics: Bristol, 2004; pp 159−292.
(17) Klika, V.; Marsik, F. Coupling effect between mechanical loading and chemical reactions. *J. Phys. Chem. B* **2009**, *113*, 14689−14697.
(18) Baláž, P. Applied Mechanochemistry. *Mechanochemistry in Nanoscience and Minerals Engineering*; Springer: Berlin/Heidelberg, 2008; pp 297−405.

DOI: 10.1021/acsomega.8b01431
ACS Omega 2018, 3, 9196−9209

(19) Delogu, F. A combined experimental and numerical approach to the kinetics of mechanically induced phase transformations. *Acta Mater.* **2008**, *56*, 905−912.
(20) Martin, C.; Bouvard, D.; Shima, S. Study of particle rearrangement during powder compaction by the Discrete Element Method. *J. Mech. Phys. Solids* **2003**, *51*, 667−693.
(21) Soni, P. R. *Mechanical alloying: fundamentals and applications*; Cambridge International Science Publishing: Cambridge, UK, 1998.
(22) Lü, L., Lai, M. O. *Mechanical alloying*; Springer: Boston, MA, 1998.
(23) Chattopadhyay, P.; Manna, I.; Talapatra, S.; Pabi, S. A mathematical analysis of milling mechanics in a planetary ball mill. *Mater. Chem. Phys.* **2001**, *68*, 85−94.
(24) Venkataraman, K.; Narayanan, K. Energetics of collision between grinding media in ball mills and mechanochemical effects. *Powder Technol.* **1998**, *96*, 190−201.
(25) Abdellaoui, M.; Gaffet, E. The physics of mechanical alloying in a planetary ball mill: mathematical treatment. *Acta Metall. Mater.* **1995**, *43*, 1087−1098.
(26) Burgio, N.; Iasonna, A.; Magini, M.; Martelli, S.; Padella, F. Mechanical alloying of the Fe−Zr system. Correlation between input energy and end products. *Nuovo Cimento Soc. Ital. Fis., D* **1991**, *13*, 459−476.
(27) Butyagin, P. Y. Kinetics and nature of mechanochemical reactions. *Russ. Chem. Rev.* **1971**, *40*, 901−915.
(28) Chen, Y.; Bibole, M.; Le Hazif, R.; Martin, G. Ball-milling-induced amorphization in NixZry compounds: a parametric study. *Phys. Rev. B: Condens. Matter Mater. Phys.* **1993**, *48*, 14−21.
(29) Cocco, G.; Delogu, F.; Monagheddu, M.; Mulas, G.; Schiffini, L. Impact characteristics and mechanical alloying processes by ball milling: experimental evaluation and modelling outcomes. *Int. J. Non-Equilibrium Process* **2000**, *11*, 235−269.
(30) Delogu, F.; Schiffini, L.; Cocco, G. The invariant laws of the amorphization processes by mechanical alloying. *Philos. Mag. A* **2001**, *81*, 1917−1937.
(31) Feng, Y. T.; Han, K.; Owen, D. R. J. Discrete element simulation of the dynamics of high energy planetary ball milling processes. *Mater. Sci. Eng., A* **2004**, *375*−*377*, 815−819.
(32) Gaffet, E.; Yousfi, L. Crystal to non-equilibrium phase transition induced by ball-milling. *Mater. Sci. Forum* **1992**, *90*, 51−58.
(33) Huang, H.; Pan, J.; McCormick, P. G. On the dynamics of mechanical milling in a vibratory mill. *Mater. Sci. Eng., A* **1997**, *232*, 55−62.
(34) Jiang, X.; Trunov, M. A.; Schoenitz, M.; Dave, R. N.; Dreizin, E. L. Mechanical alloying and reactive milling in a high energy planetary mill. *J. Alloys Compd.* **2009**, *478*, 246−251.
(35) Kakuk, G.; Zsoldos, I.; Csanády, Á.; Oldal, I. Contributions to the modelling of the milling process in a planetary ball mill. *Rev. Adv. Mater. Sci.* **2009**, *22*, 21−38.
(36) Le Brun, P.; Froyen, L.; Delaey, L. The modelling of the mechanical alloying process in a planetary ball mill: comparison between theory and in-situ observations. *Mater. Sci. Eng., A* **1993**, *161*, 75−82.
(37) Magini, M.; Iasonna, A.; Padella, F. Ball milling: an experimental support to the energy transfer evaluated by the collision model. *Scr. Mater.* **1996**, *34*, 13−19.
(38) Mio, H.; Kano, J.; Saito, F.; Kaneko, K. Effects of rotational direction and rotation-to-revolution speed ratio in planetary ball milling. *Mater. Sci. Eng., A* **2002**, *332*, 75−80.
(39) Mio, H.; Kano, J.; Saito, F.; Kaneko, K. Optimum revolution and rotational directions and their speeds in planetary ball milling. *Int. J. Miner. Process.* **2004**, *74*, S85−92.
(40) Pochet, P.; Tominez, E.; Chaffron, L.; Martin, G. Order-disorder transformation in Fe-Al under ball milling. *Phys. Rev. B: Condens. Matter Mater. Phys.* **1995**, *52*, 4006−4016.
(41) Cocco, G.; Delogu, F.; Schiffini, L. Toward a quantitative understanding of the mechanical alloying process. *J. Mater. Synth. Process.* **2000**, *8*, 167−180.
(42) Manai, G.; Delogu, F.; Rustici, M. Onset of chaotic dynamics in a ball mill: attractors merging and crisis induced intermittency. *Chaos* **2002**, *12*, 601.
(43) Caravati, C.; Delogu, F.; Cocco, G.; Rustici, M. Hyperchaotic qualities of the ball motion in a ball milling device. *Chaos* **1999**, *9*, 219−226.
(44) Burmeister, C. F.; Kwade, A. Process engineering with planetary ball mills. *Chem. Soc. Rev.* **2013**, *42*, 7660−7667.
(45) Ajaal, T.; Smith, R. W.; Yen, W. T. The development and characterization of a ball mill for mechanical alloying. *Can. Metall. Q.* **2002**, *41*, 7−14.
(46) Calka, A.; Radlinski, A. Universal high performance ball-milling device and its application for mechanical alloying. *Mater. Sci. Eng., A* **1991**, *134*, 1350−1353.
(47) Ali, M.; Bysouth, S. High throughput process of optimization of pigment concentrates. *NED University, J. Res. Appl. Sci.* **2014**, *11*, 15−23.
(48) Bysouth, S. R.; Bis, J. A.; Igo, D. Cocrystallization via planetary milling: enhancing throughput of solid-state screening methods. *Int. J. Pharm.* **2011**, *411*, 169−171.
(49) Goldman, E.; Smyth, M. S.; Bonnaud, T.; Suleiman, O.; Worrall, C. P., Co-cristaux d'un inhibiteur de la tyrosine kinase de bruton. Int. Patent WO 2016160604 A1, 2016.
(50) Martina, K.; Rotolo, L.; Porcheddu, A.; Delogu, F.; Bysouth, S. R.; Cravotto, G.; Colacino, E. High throughput mechanochemistry: application to parallel synthesis of benzoxazines. *Chem. Commun.* **2018**, *54*, 551−554.
(51) Bysouth, S. R. U.S. Patent US2006/0175443 A1, 2006. For more details visit http://www.automaxionltd.com/.
(52) Friščić, T.; Halasz, I.; Beldon, P. J.; Belenguer, A. M.; Adams, F.; Kimber, S. A. J.; Honkimäki, V.; Dinnebier, R. E. Real-time and in situ monitoring of mechanochemical milling reactions. *Nat. Chem.* **2013**, *5*, 66−73.
(53) Gracin, D.; Štrukil, V.; Friščić, T.; Halasz, I.; Užarević, K. Laboratory real-time and in situ monitoring of mechanochemical milling reactions by Raman spectroscopy. *Angew. Chem., Int. Ed.* **2014**, *53*, 6193−6197.
(54) Batzdorf, L.; Fischer, F.; Wilke, M.; Wenzel, K.-J.; Emmerling, F. Direct in situ investigation of milling reactions using combined X-ray diffraction and Raman spectroscopy. *Angew. Chem., Int. Ed.* **2015**, *54*, 1799−1802.
(55) Halasz, I.; Kimber, S. A. J.; Beldon, P. J.; Belenguer, A. M.; Adams, F.; Honkimâki, V.; Nightingale, R. C.; Dinnebier, R. E.; Friščić, T. In situ and real-time monitoring of mechanochemical milling reactions using synchrotron X-ray diffraction. *Nat. Protoc.* **2013**, *8*, 1718−1729.
(56) Kulla, H.; Haferkamp, S.; Akhmetova, I.; Rollig, M.; Maierhofer, C.; Rademann, K.; Emmerling, F. In Situ Investigations of Mechanochemical One-Pot Syntheses. *Angew. Chem., Int. Ed.* **2018**, *57*, 5930−5933.
(57) Boldyrev, V. V. Mechanochemistry and mechanical activation of solids. *Bull. Acad. Sci. USSR, Div. Chem. Sci.* **1990**, *39*, 2029−2044.
(58) *Experimental and Theoretical Studies in Modern Mechanochemistry*; Delogu, F., Mulas, G., Eds.; Transworld Research Network: Kerala, India, 2010.
(59) Gilman, J. J. Mechanochemistry. *Science* **1996**, *274*, 65−68.
(60) Gutman, E. M. *Mechanochemistry of Materials*; Cambridge International Science Publishing: Cambridge, 1998.
(61) Heinicke, G. *Tribochemistry*; Akademie Verlag: Berlin, 1984.
(62) Delogu, F.; Takacs, L. Mechanochemistry of Ti−C powder mixtures. *Acta Mater.* **2014**, *80*, 435−444.
(63) Gutman, E. M. Empiricism or self-consistent theory in chemical kinetics? *J. Alloys Compd.* **2007**, *434*−*435*, 779−782.
(64) Garroni, S.; Soru, S.; Enzo, S.; Delogu, F. Reduction of grain size in metals and metal mixtures processed by ball milling. *Scr. Mater.* **2014**, *88*, 9−12.
(65) Delogu, F. Mechanochemical behavior of surface radicals in ground quartz. *J. Phys. Chem. C* **2011**, *115*, 21230−21235.

DOI: 10.1021/acsomega.8b01431
ACS Omega 2018, 3, 9196−9209

(66) Delogu, F. A mechanistic study of $Ag_{50}Cu_{50}$ solid solution formation by mechanical alloying. *Acta Mater.* **2008**, *56*, 2344−2352.
(67) Delogu, F.; Cocco, G. Kinetics of amorphization processes by mechanical alloying: a modeling approach. *J. Alloys Compd.* **2007**, *436*, 233−240.
(68) Fischer, F.; Wenzel, K.-J.; Rademann, K.; Emmerling, F. Quantitative determination of activation energies in mechanochemical reactions. *Phys. Chem. Chem. Phys.* **2016**, *18*, 23320−23325.
(69) Halasz, I.; Puskaric, A.; Kimber, S. A. J.; Beldon, P. J.; Belenguer, A. M.; Adams, F.; Honkimäki, V.; Dinnebier, R. E.; Patel, B.; Jones, W.; Štrukil, V.; Friščić, T. Real-time in situ powder X-ray diffraction monitoring of mechanochemical synthesis of pharmaceutical cocrystals. *Angew. Chem., Int. Ed.* **2013**, *52*, 11538−11541.
(70) Lukin, S.; Stolar, T.; Tireli, M.; Blanco, M. V.; Babić, D.; Friščić, T.; Užarević, K.; Halasz, I. Tandem in situ monitoring for quantitative assessment of mechanochemical reactions involving structurally unknown phases. *Chem. - Eur. J.* **2017**, *23*, 13941−13949.
(71) Julien, P. A.; Malvestiti, I.; Friščić, T. The effect of milling frequency on a mechanochemical organic reaction monitored by in situ Raman spectroscopy. *Beilstein J. Org. Chem.* **2017**, *13*, 2160−2168.
(72) Hutchings, B. P.; Crawford, D. E.; Gao, L.; Hu, P.; James, S. L. Feedback kinetics in mechanochemistry: the Importance of cohesive states. *Angew. Chem., Int. Ed.* **2017**, *56*, 15252−15256.
(73) Boldyreva, E. Non-ambient conditions in the investigation and manufacturing of drug forms. *Curr. Pharm. Des.* **2016**, *22*, 4981−5000.
(74) Belenguer, A. M.; Lampronti, G. I.; Wales, D. J.; Sanders, J. K. M. Direct observation of intermediates in a thermodynamically controlled solid-state dynamic covalent reaction. *J. Am. Chem. Soc.* **2014**, *136*, 16156−16166.
(75) Schafer, F. P., Ed.; *Dye Lasers*; Springer Verlag: Berlin/Heidelberg, 1990.
(76) Grabowski, Z. R.; Rotkiewicz, K.; Rettig, W. Structural Changes Accompanying Intramolecular Electron Transfer: Focus on Twisted Intramolecular Charge-Transfer States and Structures. *Chem. Rev.* **2003**, *103*, 3899−4031.
(77) Verma, P.; Pal, H. Unusual H-Type Aggregation of Coumarin-481 Dye in Polar Organic Solvents. *J. Phys. Chem. A* **2013**, *117*, 12409−1241.

DOI: 10.1021/acsomega.8b01431
ACS Omega 2018, 3, 9196−9209